

## Measurements of CKM angle $\gamma$ in LHCb

---

**Martin Tat**<sup>a,\*</sup>

<sup>a</sup>*University of Oxford,  
Keble Road, OX1 3RH, Oxford, United Kingdom*

*E-mail:* [martin.tat@cern.ch](mailto:martin.tat@cern.ch)

In these proceedings, the current status of measurements of the CKM angle  $\gamma$  at LHCb is presented. The combination of the current measurements by LHCb to date is discussed, as well as results that are not yet included in the combination. This includes a first measurement of  $\gamma$  using the  $B^\pm \rightarrow Dh^\pm$  decay with  $D \rightarrow K^+K^-\pi^+\pi^-$ , where  $h = \pi, K$ . This analysis uses charm strong-phase parameters predicted by a model, but it will be updated when direct measurements of these parameters is available. In addition, two model-independent measurements of  $\gamma$  using the charm decays  $D \rightarrow K_S^0\pi^+\pi^-$  and  $D \rightarrow K_S^0K^+K^-$  are shown for the first time, using the channels  $B^0 \rightarrow DK^*$  and  $B^\pm \rightarrow D^*h^\pm$ . Finally, future prospects are discussed.

*20th International Conference on B-Physics at Frontier Machines (Beauty2023)  
3-7 July, 2023  
Clermont-Ferrand, France*

---

\*Speaker

## 1. Introduction

In the Standard Model (SM), the interactions between up- and down-type quarks are described by the Cabibbo–Kobayashi–Maskawa (CKM) matrix [1, 2]. The CKM matrix is unitary, which imposes several constraints on the matrix elements. They can be visualised on the complex plane as a closed triangle, known as the Unitary Triangle (UT) [3]. The level of  $CP$ -violation in the SM is proportional to the area of the UT. To fully understand  $CP$ -violation, the lengths and angles of the UT must be precisely measured.

The CKM angle  $\gamma$  is the only angle of the UT that can be measured in tree-level decays, using the interference of the  $b \rightarrow c\bar{u}s$  and  $b \rightarrow u\bar{c}s$  transitions. Experimentally,  $\gamma$  can be measured directly with negligible theoretical uncertainties [4], making it an ideal standard candle for the SM, and it can be compared with measurements of other angles and lengths of the UT. By overconstraining the UT, hints towards physics beyond the SM could be revealed.

A suitable decay is  $B^\pm \rightarrow DK^\pm$ , which is a superposition of  $B^\pm \rightarrow D^0K^\pm$  and  $B^\pm \rightarrow \bar{D}^0K^\pm$ . Furthermore, similar  $B$  decays, such as  $B^\pm \rightarrow D^*K^\pm$  and  $B^0 \rightarrow DK^*$ , also exhibit the same type of interference effects. To obtain the best possible precision on  $\gamma$ , LHCb has combined the individual  $\gamma$  measurements, and the combined result is  $\gamma = (63.8^{+3.5}_{-3.7})^\circ$  [5].

## 2. Measurement strategy

In the decay  $B^\pm \rightarrow DK^\pm$ , the two decay paths have a strong-phase difference  $\delta_B$  and a weak-phase difference  $\gamma$ . The decay  $B^\pm \rightarrow \bar{D}^0K^\pm$  is suppressed, relative to  $B^\pm \rightarrow D^0K^\pm$ , due to colour and CKM matrix elements. The magnitude of this suppression is parameterised by  $r_B$ . The decay rate of the  $B^-$  decay can thus be expressed as a coherent sum of these decay paths,

$$\mathcal{A}(B^-) = \mathcal{A}_B \left( \mathcal{A}_{D^0} + r_B e^{i(\delta_B - \gamma)} \mathcal{A}_{\bar{D}^0} \right),$$

where  $\mathcal{A}$  are decay amplitudes. Under a  $CP$  transformation, the weak phase  $\gamma$  changes sign, resulting in a different a different decay rate for the corresponding  $B^+$  decay. To study  $CP$  violation and measure  $\gamma$ , one must therefore compare the yield of  $B^+$  and  $B^-$  decays.

In these proceedings, the focus will be on self-conjugate multi-body  $D$ -decay final states. These decays have a complex resonance structure and the decay amplitudes vary as a function of the phase-space position. Therefore, in addition to the strong-phase difference  $\delta_B$ , there is also a charm strong-phase difference  $\delta_D$  between the  $D^0$  and  $\bar{D}^0$  decay amplitudes.

Since  $\delta_D$  varies across phase space, knowledge of this charm strong-phase difference is required in order to interpret  $\gamma$  from the measured asymmetries between  $B^+$  and  $B^-$  decays. While  $\delta_D$  can be determined from an amplitude model, it is desirable to use external model-independent inputs. For the decays  $D \rightarrow K_S^0 \pi^+ \pi^-$  and  $D \rightarrow K_S^0 K^+ K^-$ , the strong-phase differences have been measured in bins of phase space, using a binning scheme optimised for the measurement of  $\gamma$  [6]. The binning scheme can be visualised on a Dalitz plot, shown on the top of Fig. 1.

## 3. Phase-space binned analysis of $B^\pm \rightarrow [K^+ K^- \pi^+ \pi^-]_D K^\pm$

The decay  $D \rightarrow K^+ K^- \pi^+ \pi^-$  can be analysed with a procedure analogous to that of  $D \rightarrow K_S^0 h^+ h^-$ . Using an amplitude model to predict the strong-phase difference  $\delta_D$  [7], the five-dimensional phase

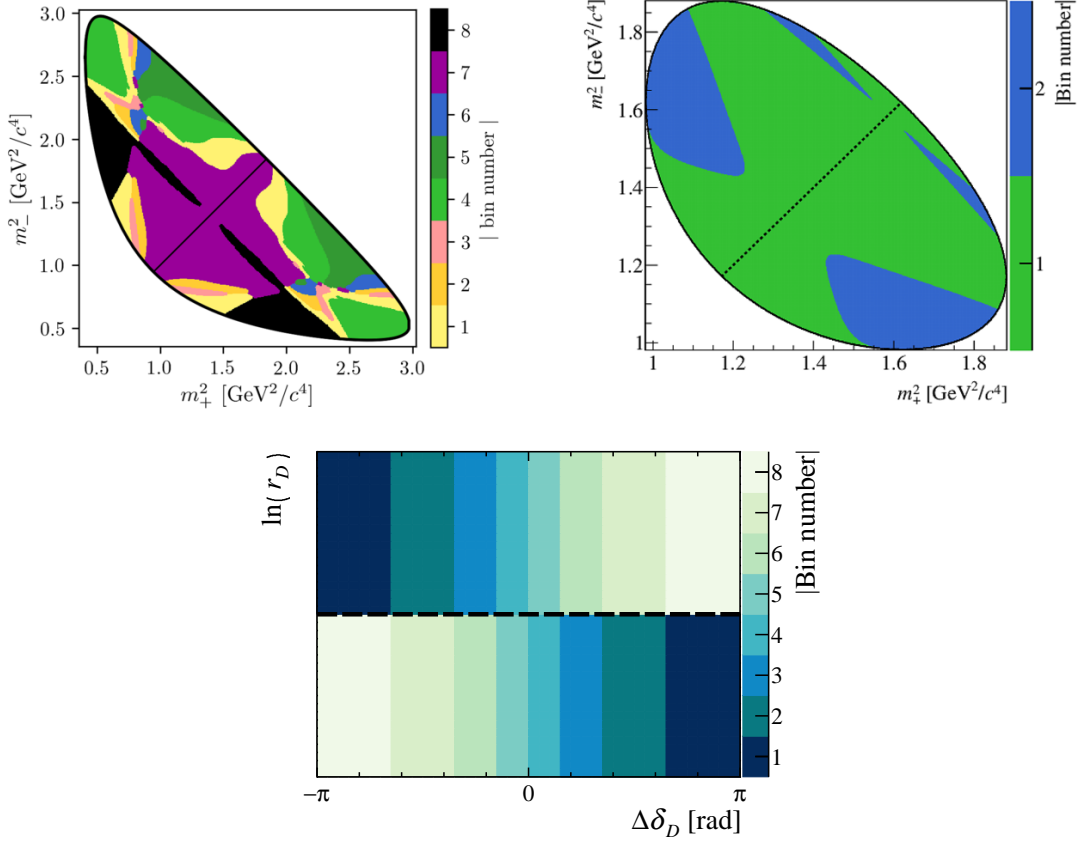


**Figure 1:** Binning schemes of the charm decays  $D \rightarrow K_S^0 \pi^+ \pi^-$  (top left),  $D \rightarrow K_S^0 K^+ K^-$  (top right) and  $D \rightarrow K^+ K^- \pi^+ \pi^-$  (bottom).

space is divided into eight bins, as shown at the bottom of Fig. 1. In the current analysis, the amplitude-averaged strong-phases are calculated from the amplitude model.

To identify the signal shape and constrain backgrounds, the invariant  $B^\pm$  mass spectrum is fitted, as shown in Fig. 2. In total,  $3026 \pm 38$  ( $44349 \pm 218$ ) signal candidates are found in the  $B^\pm \rightarrow DK^\pm$  ( $D\pi^\pm$ ) channel. Finally, the  $B^\pm$  candidates are split by charge and phase-space bins, and the number of  $B^\pm \rightarrow Dh^\pm$  candidates are fitted in each fit category. The asymmetries in phase-space bins are shown on the left in Fig. 3. Non-zero bin asymmetries are seen in most bins, and the change in asymmetries across bins is driven by the variation in strong-phase differences.

The signal yields are interpreted in terms of  $\gamma$ , as shown on the right in Fig. 3. The fit results are  $\gamma = (116_{-14}^{+12})^\circ$ ,  $\delta_D^{DK} = (81_{-14}^{+12})^\circ$  and  $r_B^{DK} = 0.110_{-0.020}^{+0.020}$ . Note that currently, these values are interpreted using model-predicted values of charm strong-phases, and they may evolve when updated using model-independent inputs.

#### 4. Neutral $B$ decays

The CKM angle  $\gamma$  may also be measured in neutral  $B^0$  decays, but the branching fraction of the  $B^0 \rightarrow DK^*$  decay is lower than that of  $B^\pm \rightarrow DK^\pm$ . However, the suppressed  $B^0 \rightarrow D^0 K^*$  channel

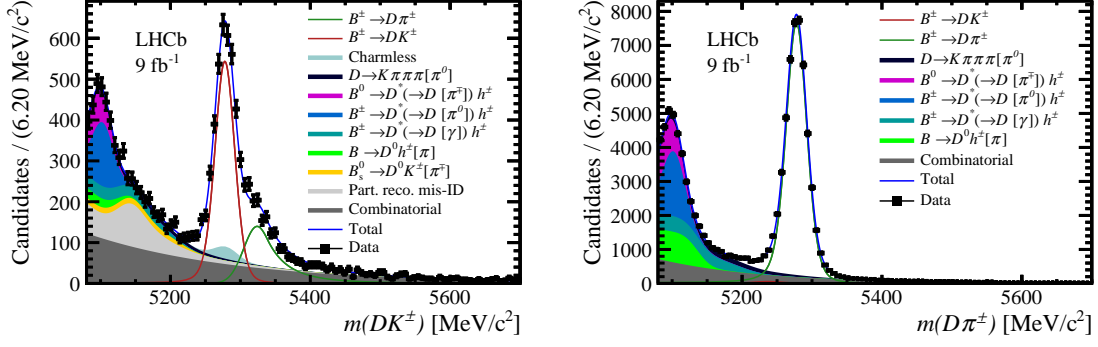


**Figure 2:** Invariant-mass fits to the  $B^\pm \rightarrow Dh^\pm$  channels. The data are shown as black points with error bars and the full fit model is the blue curve.

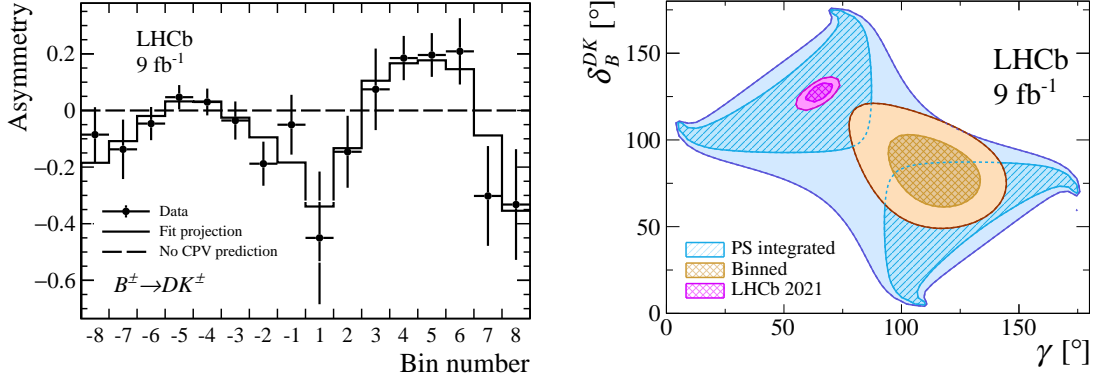


**Figure 3:** Left: The fractional bin asymmetries for the decay  $B^\pm \rightarrow [K^+K^-\pi^+\pi^-]_D K^\pm$ , which are shown as data points. The solid line is the prediction from the fitted parameters.. Rights: Interpretation of  $\gamma$  and  $\delta_B^{DK}$ .

does not have a colour suppression, relative to the favoured  $B^0 \rightarrow \bar{D}^0 K^*$  channel. Therefore, the interference effects in the  $B^0$  system are expected to be three times larger than the  $B^\pm$  system.

The analysis considers the subsequent charm decays  $D \rightarrow K_S \pi^+ \pi^-$  and  $D \rightarrow K_S^0 K^+ K^-$ , and the binning schemes on the top of Fig. 1 are used. The invariant-mass fits are shown in Fig. 4. The  $K_S^0$  meson can either decay inside the VELO, shown on the left, or downstream of the VELO, shown on the right. A large yield of the decay  $B_s^0 \rightarrow DK^*$  is also seen on the right of the signal peak, but  $CP$ -violation effects are expected to be small in this mode and are therefore not studied.

In a procedure similar to that of the  $B^\pm$  decays, the  $CP$ -violation effects are studied in each phase-space bin, and the bin asymmetries are shown on the left in in Fig. 5. The interpretation of  $\gamma$  is shown on the right in Fig. 5, and the results are  $\gamma = (49 \pm 20)^\circ$ ,  $\delta_{B^0} = (236 \pm 19)^\circ$  and  $r_{B^0} = 0.27 \pm 0.07$ , which is consistent with the LHCb combination.

## 5. $B$ decays to excited $D^*$ final states

The decay  $B^\pm \rightarrow D^* K^\pm$  is similar to the decay  $B^\pm \rightarrow DK^\pm$ , with an excited  $D^*$  meson that can decay via two channels,  $D^* \rightarrow D^0 \pi^0$  and  $D^* \rightarrow D^0 \gamma$ . Due to the opposite  $CP$  eigenvalues of  $\pi^0$

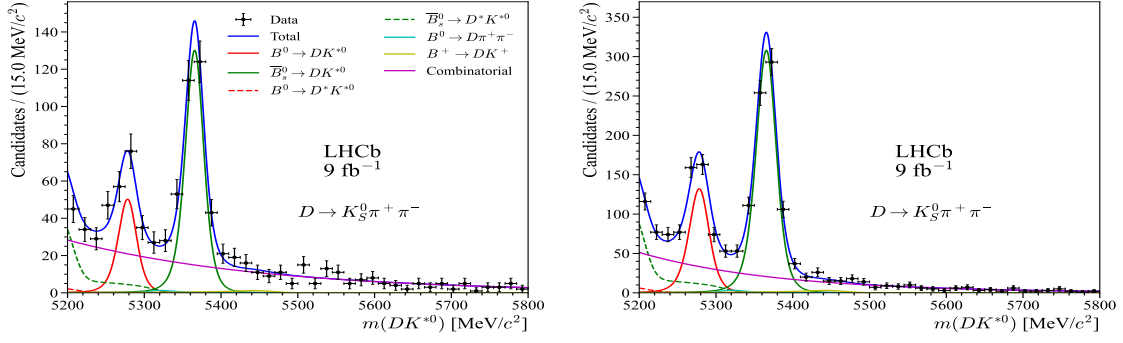


**Figure 4:** The  $B^0 \rightarrow DK^*$  invariant-mass fit, with long tracks on the left and downstream tracks on the right.

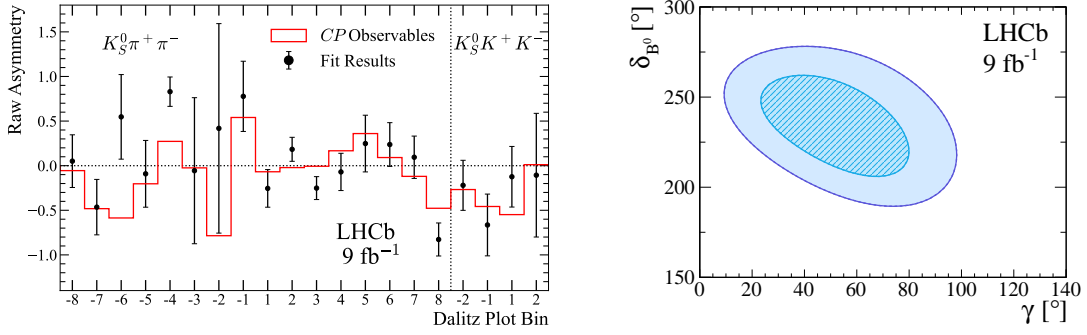


**Figure 5:** Left: Bin asymmetries in the  $B^0 \rightarrow DK^*$  decay mode, where  $D \rightarrow K_S^0 \pi^+ \pi^-$  and  $D \rightarrow K_S^0 K^+ K^-$ . Right: The fitted  $CP$ -violating observables (left) and the interpretation of  $\gamma$  (right).

and  $\gamma$ , the asymmetries between these two modes are also expected to be equal and opposite. This analysis considers the three-body charm decays  $D \rightarrow K_S^0 h^+ h^-$ .

To separate the two  $D^*$  decay channels, and to identify the complex set of backgrounds, a two-dimensional fit is performed using the reconstructed  $D^*$  mass and the invariant  $DK^\pm$  mass. The fit projection is shown in Fig. 6. The signal shape of the  $D\pi^0$  channel has a distinct double-peak structure, while the  $D\gamma$  mode has a wider peak.

The invariant-mass fit is repeated separately for each charge and phase-space bin, and the signal yields in each category are interpreted in terms of  $\gamma$ . The results are  $\gamma = (69 \pm 14)^\circ$ ,  $\delta_B^{D^*K} = (311 \pm 15)^\circ$  and  $r_B^{D^*K} = 0.15 \pm 0.03$ , which is in agreement with the current world average.

## 6. Summary and future prospects

LHCb has performed a large number of  $\gamma$  measurements, using a wide range of  $B$  and  $D$  decays. The current combination results in  $\gamma = (63.8^{+3.5}_{-3.7})^\circ$ , and three additional measurements are presented, which will be included in future combinations. The four-body decay  $D \rightarrow K^+ K^- \pi^+ \pi^-$  is studied for the first time in  $\gamma$  measurements using the decay  $B^\pm \rightarrow DK^\pm$ . This result will be updated in the future with model-independent charm strong-phase inputs. The decays  $B^0 \rightarrow DK^*$  and  $B^\pm \rightarrow D^* K^\pm$  are analysed using the  $D \rightarrow K_S^0 h^+ h^-$  channels, and the model-independent values of  $\gamma$  were found to be in perfect agreement with the current LHCb combination.

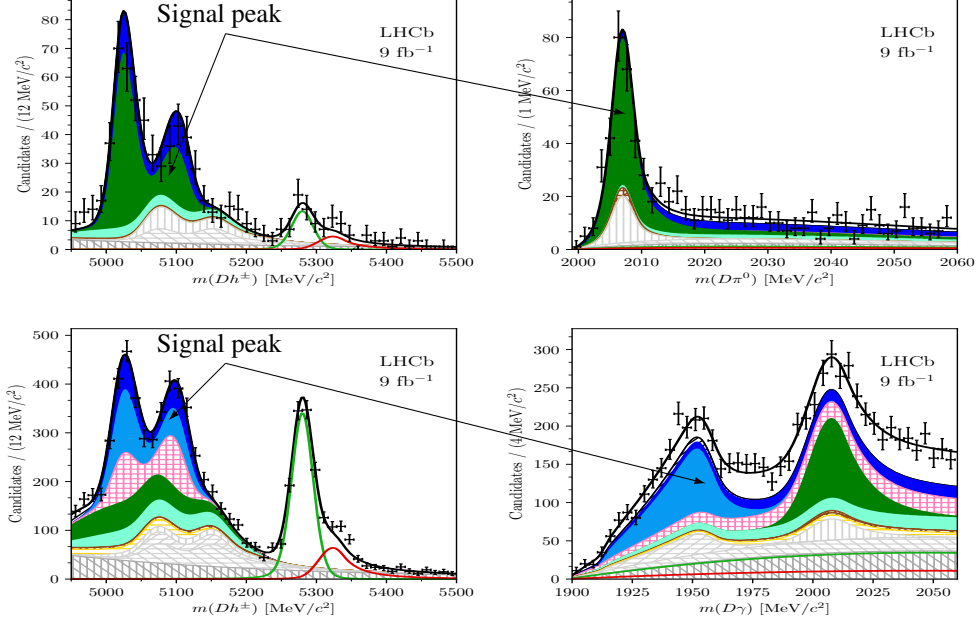


**Figure 6:** Projections of the invariant mass fit of  $B^\pm \rightarrow D^* K^\pm$ , with the  $DK^\pm$  invariant mass on the left and the  $D^*$  invariant mass on the right. The  $D\pi^0$  mode is shown on the top and the  $D\gamma$  mode is at the bottom.

The measurements are currently statistically limited, and will benefit from the large dataset anticipated for Run 3. LHCb is also expected to provide updated measurements of  $\gamma$  with the  $B_s^0$  system, and it will be interesting to compare the results with those from the  $B^\pm$  and  $B^0$  systems.

## References

- [1] N. Cabibbo, *Unitary symmetry and leptonic decays*, Phys. Rev. Lett. **10** (1963) 531
- [2] M. Kobayashi and T. Maskawa, *CP-violation in the renormalizable theory of weak interaction*, Prog. Theor. Phys. **49** (1973) 652
- [3] L. Wolfenstein, *Parametrization of the Kobayashi-Maskawa Matrix*, Phys. Rev. Lett. **51** (1983) 1945
- [4] J. Brod and J. Zupan, *The ultimate theoretical error on  $\gamma$  from  $B \rightarrow DK$  decays*, JHEP **01** (2014) 051
- [5] LHCb Collaboration, *Simultaneous determination of the CKM angle  $\gamma$  and parameters related to mixing and CP-violation in the charm sector*, LHCb Implications Workshop, October 2022
- [6] M. Ablikim et al., *Model-independent determination of the relative strong-phase difference between  $D^0$  and  $\bar{D}^0 \rightarrow K_{S,L}^0 \pi^+ \pi^-$  and its impact on the measurement of the CKM angle  $\gamma/\phi_3$* , Phys. Rev. **D101** (2020) 112002
- [7] R. Aaij et al., *Search for CP violation through an amplitude analysis of  $D^0 \rightarrow K^+ K^- \pi^+ \pi^-$  decays*, JHEP **02** (2019) 126